2-12-2022

Recurrent KRAS mutations are early events in the development of papillary renal neoplasm with reverse polaritu

Khaleel I. Al-Obaidy

Rola M. Saleeb

Kiril Trpkov

Sean R. Williamson

Ankur R. Sangoi

See next page for additional authors

Recommended Citation

Al-Obaidy KI, Saleeb RM, Trpkov K, Williamson SR, Sangoi AR, Nassiri M, Hes O, Montironi R, Cimadamore A, Acosta AM, Alruwaii ZI, Alkashash A, Hassan O, Gupta N, Osunkoya AO, Sen JD, Baldrige LA, Sakr WA, Idrees MT, Eble JN, Grignon DJ, and Cheng L. Recurrent KRAS mutations are early events in the development of papillary renal neoplasm with reverse polarity. Mod Pathol 2022.

Authors

Khaleel I. Al-Obaidy, Rola M. Saleeb, Kiril Trpkov, Sean R. Williamson, Ankur R. Sangoi, Mehdi Nassiri, Ondrej Hes, Rodolfo Montironi, Alessia Cimadamore, Andres M. Acosta, Zainab I. Alruwaii, Ahmad Alkashash, Oudai Hassan, Nilesh S. Gupta, Adeboye O. Osunkoya, Joyashree D. Sen, Lee Ann Baldrige, Wael A. Sakr, Muhammad T. Idrees, John N. Eble, David J. Grignon, and Liang Cheng

www.nature.com/modpathol

ARTICLE

Recurrent *KRAS* mutations are early events in the development of papillary renal neoplasm with reverse polarity

Khaleel I. Al-Obaidy[1], Rola M. Saleeb[2,13], Kiril Trpkov[3], Sean R. Williamson[1], Ankur R. Sangoi[4], Mehdi Nassiri[5,13], Ondrej Hes[6], Rodolfo Montironi[7], Alessia Cimadamore[7], Andres M. Acosta[8], Zainab I. Alruwaii[9], Ahmad Alkashash[5], Oudai Hassan[10], Nilesh Gupta[10], Adeboye O. Osunkoya[11], Joyashree D. Sen[5], Lee Ann Baldrige[5], Wael A. Sakr[12], Muhammad T. Idrees[2], John N. Eble[5], David J. Grignon[5,13] and Liang Cheng[5]✉

We evaluated the clinicopathologic and molecular characteristics of mostly incidentally detected, small, papillary renal neoplasms with reverse polarity (PRNRP). The cohort comprised 50 PRNRP from 46 patients, divided into 2 groups. The clinically undetected (<5 mm) neoplasms ($n = 34$; 68%) had a median size of 1.1 mm (range 0.2–4.3 mm; mean 1.4 mm), and the clinically detected (≥5 mm) neoplasms ($n = 16$; 32%) which had a median size of 13 mm (range 9–30 mm; mean 16 mm). Neoplasms were positive for GATA3 (n = 47; 100%) and L1CAM ($n = 34/38$; 89%) and were negative for vimentin ($n = 0/44$; 0%) and, to a lesser extent, AMACR [($n = 12/46$; 26%; weak = 9, weak/moderate = 3)]. *KRAS* mutations were found in 44% ($n = 15/34$) of the clinically undetected PRNRP and 88% of the clinically detected PRNRP ($n = 14/16$). The two clinically detected PRNRP with wild-type *KRAS* gene were markedly cystic and contained microscopic intracystic tumors. In the clinically undetected PRNRP, the detected *KRAS* mutations rate was higher in those measuring ≥1 mm vs <1 mm [n = 14/19 (74%) vs n = 1/15 (7%)]. Overall, the *KRAS* mutations were present in exon 2—codon 12: c.35 G > T ($n = 21$), c.34 G > T ($n = 3$), c.35 G > A ($n = 2$), c.34 G > C ($n = 2$) resulting in p.Gly12Val, p. Gly12Asp, p.Gly12Cys and p.Gly12Arg, respectively. One PRNRP had a G12A/V/D complex mutation. Twenty-six PRNRP were concurrently present with other tumors of different histologic subtypes in the ipsilateral kidney; molecular testing of 8 of the latter showed wild-type *KRAS* gene despite the presence of *KRAS* mutations in 5 concurrent PRNRP. On follow up, no adverse pathologic events were seen (range 1–160 months; mean 44 months). In conclusion, the presence of *KRAS* mutations in small, clinically undetected PRNRP provides a unique finding to this entity and supports its being an early event in the development of these neoplasms.

Modern Pathology; https://doi.org/10.1038/s41379-022-01018-6

INTRODUCTION

In 2019, we described a distinct subset of epithelial renal neoplasms "papillary renal neoplasm with reverse polarity" (PRNRP) that was characterized by papillary or tubulopapillary architectures, with delicate fibrovascular cores lined by a single layer of eosinophilic cells with finely granular cytoplasm, which had apically located round nuclei with inconspicuous nucleoli. PRNRP was uniformly positive for GATA3 and L1CAM and negative for vimentin and, to a lesser extent, α-methylacyl-CoA-racemase (AMACR/p504s) by immunohistochemistry[1]. Furthermore, we demonstrated that these tumors harbor recurrent *KRAS* mutations, which are not known to occur in other types of renal epithelial neoplasms[2]. Genitourinary Pathology Society (GUPS) has considered PRNRP in its recent update on existing renal neoplasms to represent a distinct pattern/subtype within the spectrum of papillary RCC, indicating that additional studies are needed to further validate it[3]. Cases with similar or identical morphology to PRNRP have been described in earlier studies as "papillary renal cell carcinoma with oncocytic cells and nonoverlapping low-grade nuclei"[4] and "papillary renal cell carcinoma type 4/ oncocytic low grade"[5], based on their distinct morphology and similar or identical immunoprofile. More recently, several reports have also been published on this entity, reinforcing our morphologic and molecular findings[6–12].

In our examination of resected end-stage kidneys, we found small clinically undetected lesions (<5 mm) that were morphologically identical to the PRNRP. These lesions were previously called papillary adenoma type 2, or, more recently, type D[13,14]. In a prior molecular interrogation of a limited number of samples, we identified recurrent *KRAS* mutations in 3 of these small lesions[15]. In the current study, we

[1]Robert J Tomsich Pathology and Laboratory Medicine Institute, Cleveland Clinic, Cleveland, OH, USA. [2]Department of Laboratory Medicine and Pathobiology, University of Toronto, Toronto, ON, Canada. [3]Department of Pathology and Laboratory Medicine, Cumming School of Medicine, University of Calgary, Calgary, AB, Canada. [4]Department of Pathology, El Camino Hospital, Mountain View, CA, USA. [5]Department of Pathology and Laboratory Medicine, School of Medicine, Indiana University, Indianapolis, IN, USA. [6]Department of Pathology, Charles University in Prague, Faculty of Medicine and University Hospital in Plzen, Plzen, Czech Republic. [7]Section of Pathological Anatomy, School of Medicine, United Hospitals, Marche Polytechnic University, Ancona, Italy. [8]Women's and Perinatal Pathology, Department of Pathology, Brigham and Women's Hospital, Harvard Medical School, Boston, MA, USA. [9]Department of Pathology, Regional Laboratory and Blood Bank, Eastern Province, Dammam, Saudi Arabia. [10]Department of Pathology and Laboratory Medicine, Henry Ford Hospital, Detroit, MI, USA. [11]Department of Pathology, Emory University School of Medicine, Atlanta, GA, USA. [12]Department of Pathology, Wayne State University/ Detroit Medical Center, Detroit, MI, USA. [13]Deceased: David J. Grignon ✉email: liang_cheng@yahoo.com

Received: 16 November 2021 Revised: 21 January 2022 Accepted: 21 January 2022
Published online: 12 February 2022

analyzed the immunohistochemical characteristics and performed targeted polymerase chain reaction for *KRAS* mutations on an expanded cohort of PRNRP.

MATERIALS AND METHODS

Study population and case selection

The files of the pathology departments at the participating institutions were searched for lesions that fulfilled our previously suggested diagnostic criteria for papillary renal neoplasm with reverse polarity (PRNRP)[1]. A series of 177 end-stage renal disease specimens from the Indiana University Health archives were reviewed in search of small lesions that resembled PRNRP. Additionally, kidney resection specimens with a diagnosis of papillary adenoma were also re-examined in search of these neoplasms by one of the authors (KIA). A search of additional material from our previous cohort[1] identified sufficient tissue for further analysis in three cases (corresponding to tumors 3, 9, and 16 of the original study). The cases selected for inclusion in the study were divided into small/ clinically undetected [size <5 mm (radiologically and/or grossly undetected –incidental/microscopic-)] and large/ clinically detected [size ≥5 mm (radiologically and/or grossly detected –non-incidental)] neoplasms.

Due to the shared positive immunohistochemical reaction for GATA3[16], 10 randomly selected clear cell papillary renal cell carcinomas, were retrieved from the pathology archives at Indiana University.

Histopathologic study

Tissues from all tumors were fixed in 10% neutral buffered formalin and embedded in paraffin. Sections of 4 µm thickness were stained with hematoxylin and eosin. Based on our previous study[1] and other published reports, as recently summarized by Wei et al.[10], a panel of 4 differentiating antibodies between PRNRP and PRCC was utilized. These were directed against GATA3 (L50-829; Biocare Medical, Pacheco, CA), L1CAM (UJ127; Sigma-Aldrich, St. Louis, MO), vimentin (V9; Dako) and α-methylacyl-CoA-racemase (AMACR/p504S [13H4; Dako]) and utilized in a Dako automated instrument. Positive and negative controls provided appropriate results for each stain. The staining was recorded as negative (–) or positive (+), the latter indicating a diffuse and strong reaction. For tumors with positive reactions other than strong and diffuse, weak (w) or moderate (m) intensity was recorded.

KRAS mutational analysis

A targeted polymerase chain reaction analysis was performed as previously described[17]. Briefly, formalin-fixed, paraffin-embedded tissue blocks were retrieved from each of the 50 neoplasms. DNA extraction from the microdissected tumors areas from 4 um cut slides was performed using the Qiagen QIAamp DNA FFPE Tissue Kit (Qiagen, Valencia, CA, USA). DNA concentration was determined using the NanoDrop Spectrophotometer and adjusted to ~10 ng/µl in ddH_2O. Polymerase chain reaction testing was performed according to the recommended procedure using the Qiagen therascreen *KRAS* RGQ PCR Kit on the Qiagen Rotor-Gene Q MDx instrument. The therascreen *KRAS* RGQ PCR Kit provides eight separate PCR amplification reactions: seven mutation-specific reactions in codons 12 and 13 of exon 2 of the *KRAS* oncogene [Gly12Ala (G12A), Gly12Asp (G12D), Gly12Arg (G12R), Gly12Cys (G12C), Gly12Ser (G12S), Gly12Val (G12V), and Gly13Asp (G13D)] and a wild-type control in exon 4. Analysis of crossing thresholds and mutation calls for each PCR amplification reaction was performed by the Rotor-Gene Q therascreen *KRAS* Assay analysis software once runs were completed. *KRAS* analysis was also performed on the clear cell papillary renal cell carcinomas, the concurrent ipsilateral renal tumors of different or similar morphologies, and to 4 "mimickers" described in the original series[1].

RESULTS

Clinical and pathologic features

The clinical and pathologic features are tabulated in Tables 1 and 2. The clinically undetected neoplasms constituted 68% ($n = 34/50$) and ranged from 0.2 to 4.3 mm (mean 1.4 mm, median 1.2 mm). All were diagnosed on nephrectomy (27 total and 7 partial) specimens performed either for end-stage kidney disease (n = 12/34; 35%) or for concurrent ipsilateral tumor ($n = 23/34$; 68%) with/or without end-stage kidney disease. The clinically detected ones constituted 32% ($n = 16/50$) and ranged from 9 to 30 mm (mean 16 mm, median 13 mm). All, except one ($n = 15/16$), were diagnosed on nephrectomy (5 total and 10 partial) specimens performed for radiologically detected neoplasms, with the last case being diagnosed on biopsy. Concurrent ipsilateral tumors were present in 3 cases. All neoplasms were staging category pT1a and showed low nucleolar grade [International Society of Urological Pathology/ WHO (ISUP/WHO) grades 1–2]. On follow-up, all patients with available follow-up had a benign neoplasm-related clinical course (range 1–160 months, mean 44 months, median 30 months), although 5 patients died of other causes.

Morphologically, both groups of neoplasms shared similar morphologic features as previously described[1]. However, in addition to the commonly described features, cystic expansion with intracystic papillary proliferation was seen in 7 of the clinically detected (≥5 mm) neoplasms. These were filled with eosinophilic proteinaceous material that contained loose macrophages with or without hemosiderin deposits and cellular debris (Fig. 1A). Although the majority of neoplasms were composed of thin cores of arborizing papillary, or less frequently, tubulopapillary, architecture, 3 of the clinically detected neoplasms had edematous and focally fibrotic papillary cores, these frequently contained chronic inflammatory infiltrates (Fig. 1B). Cytologically, the cells were mostly cuboidal cells with eosinophilic finely granular cytoplasm; focal areas of clear cell changes were seen in 3 neoplasms (Fig. 1C). The nuclei were characteristically located at the apical surface opposite to the basement membrane with smooth overlying luminal borders, with hobnail conformation present in 3 neoplasms (Fig. 1D). As we described before, the nuclei were mostly small, non-overlapping with regular contours, frequent nuclear clearing, inconspicuous nucleoli and had only rare areas of wrinkled nuclear contours. Focal areas of conspicuous basophilic nucleoli were seen in the areas of nuclear clearing, however, large prominent and eosinophilic nucleoli (WHO/ISUP nucleolar grade 3) were not seen. Psammoma bodies, intracellular hemosiderin, coagulative-type tumor necrosis, or mitotic figures were absent in all neoplasms.

Immunohistochemically, all evaluated neoplasms showed positive reactions for GATA3 ($n = 47/47$; 100%) (strong in 46 and weak to moderate in 1). Reactions for L1CAM were positive in 89% of the neoplasms [$n = 34/38$ (strong in 29 and weak in 5)]. Reactions for vimentin were negative in all neoplasms ($n = 0/46$; 0%) while reactions for AMACR were mostly negative ($n = 34/46$; 74%), however, 20% ($n = 9/46$) showed weak "blush-like" reactions and 3 ($n = 3/46$; 6%) showed weak to moderate reactions. In these neoplasms, the AMACR reaction had a similar intensity to that seen in the distal convoluted tubules of the kidney (Fig. 2). Interestingly, clear cell papillary renal cell carcinoma tumors showed positive reaction for GATA3 in 80% ($n = 8/10$); however, in contrast with PRNRP, they were consistently positive for vimentin ($n = 10/10$; 100%) and negative for L1CAM ($n = 0/10$; 0%).

KRAS mutational analysis

KRAS mutations were found in 44% ($n = 15/34$) of the clinically undetected (microscopic) PRNRP. The detected *KRAS* mutation rate was higher [$n = 14/19$ (74%)] in those measuring 1–5 mm than those measuring <1 mm, where only one PRNRP (measuring 0.6 mm) was positive for *KRAS* mutation [$n = 1/15$ (7%)] (Fig. 3). Of the clinically detected PRNRP, 88% ($n = 14/16$) had *KRAS* mutations with the 2 negative neoplasms being markedly cystic and contained small microscopic intracystic tumors. Overall, *KRAS* mutations were in codon 12: c.35 G > T (n = 21), c.34 G > T ($n = 3$), c.35 G > A ($n = 2$), c.34 G > C ($n = 2$) resulting in p.Gly12Val, p. Gly12Asp, p.Gly12Cys and p.Gly12Arg, respectively. One PRNRP had a G12A/V/D complex mutation (Table 3).

No *KRAS* mutations were found either in the clear cell papillary renal cell carcinomas, in 8 of the concurrent ipsilateral tumors of different histology, or the mimickers of PRNRP, included in our previous report[1].

Table 1. Detailed clinicopathologic data of the 50 papillary renal neoplasms with reverse polarity included in this cohort.

	Gender	Procedure	Age	Laterality	ESRD/ CKD	Size (mm)	KRAS status	Multiple tumors	Assocaited tumor type (Size; KRAS status)	Outsome	Follow up duration (Months)	Immunohistochemistry			
												GATA-3	L1CAM	VIMENTIN	AMACR
1	F	Partial Nehprectomy	48	Right	N	14	G12A/V/D complex mutation	N	–	NED	25	+	+	–	–
2	M	Partial Nehprectomy	45	–	N	10	p.G12V (c.35 G > T)	N	–	NED	84	+	+	–	–
3	F	Total nephrectomy	52	Left	Y	1.6	p.G12V (c.35 G > T)	Y	PRCC (2 CM)	NED	20	+	+	–	–
4	=	=	=	Right	=	1.4	p.G12V (c.35 G > T)	=	PRCC (3.5 CM)	=	=	+	–	–	–
5	M	Total nephrectomy	42	Right	Y	0.7	ND	Y	PRCC (1.5 CM)	NED	160	+	NP	NP	NP
6	M	Total nephrectomy	60	Left	Y	1.4	p.G12V (c.35 G > T)	Y	PRCC (3.8 CM)	DOC	113	NP	NP	NP	NP
7	=	=	=	=	=	1.9	p.G12C (c.34 G > T)	=	=	=	=	+	+	–	–
8	=	=	=	=	=	28	p.G12V (c.35 G > T)	=	=	=	=	+	+	–	–
9	M	Total nephrectomy	64	Right	Y	0.9	ND	Y	PA (0.5 CM)	DOC	45	+	w	–	–
10	M	Partial Nehprectomy	54	Right	N	1.4	ND	Y	CCRCC (2 CM)	NED	134	+	w	–	–
11	F	Total nephrectomy	63	Left	N	1.1	p.G12V (c.35 G > T)	Y	Oncocytoma (4.2 cm)	NED	114	+	w	–	–
12	M	Total nephrectomy	56	Right	N	2.1	p.G12D (c.35 G > A)	Y	CCRCC (7.8 cm)	NED	105	+	–	–	–
13	M	Partial Nehprectomy	65	Left	N	1	p.G12C (c.34 G > T)	Y	CCRCC (4.7 cm)	–	–	+	w	–	–
14	M	Total nephrectomy	75	Right	Y	0.6	ND	Y	ACD-RCC (2.4 cm; KRAS wild-type); PRNRP (0.8 cm; KRAS mutated)	NED	7	+	+	–	–
15	F	Total nephrectomy	54	Right	Y	10	p.G12V (c.34 G > T)	N	–	NED	35	+	+	–	w
16	F	Total nephrectomy	77	–	N	2.1	p.G12V (c.35 G > T)	Y	Multiple oncocytomas (KRAS wild-type)	NED	84	+	NP	–	w
17	F	Total nephrectomy	70	Left	Y	1.2	ND	Y	Oncocytoma (1.0 cm)	NED	87	+	NP	–	–
18	M	Total nephrectomy	52	Right	Y	0.9	ND	N	–	NED	80	w	NP	–	–

Table 1. continued

	Gender	Procedure	Age	Laterality	ESRD/ CKD	Size (mm)	KRAS status	Multiple tumors	Assocaited tumor type (Size; KRAS status)	Outsome	Follow up duration (Months)	Immunohistochemistry			
												GATA-3	L1CAM	VIMENTIN	AMACR
19	M	Total nephrectomy	76	Left	N	2.8	p.G12V (c.35 G > T)	Y	PRCC (6.5 cm)	NED	87	+	NP	–	–
20	F	Total nephrectomy	51	–	Y	16	p.G12V (c.35 G > T)	N	–	NED	60	+	NP	–	–
21	F	Total nephrectomy	54	Right	Y	0.4	ND	N	–	NED	60	+	+	–	–
22	M	Partial Nehprectomy	77	Left	N	0.6	ND	Y	CCRCC (6 CM); CCPRCC (0.6 CM)	DOC	5	+	w	–	w
23	F	Partial Nehprectomy	56	–	N	11	p.G12V (c.35 G > T)	N	–	NED	75	+	NP	NP	NP
24	F	Total nephrectomy	84	Right	Y	0.8	ND	N	–	NED	24	+	–	–	–
25	F	Total nephrectomy	72	Left	Y	1.4	p.G12V (c.35 G > T)	N	–	DOC	9	+	+	–	–
26	F	Total nephrectomy	33	Left	Y	0.8	ND	N	–	NED	52	+	+	–	–
27	F	Total nephrectomy	73	Right	Y	0.9	ND	Y	ACD-RCC (3.6 cm; KRAS wild-type); URCC (5.5 cm)	–	–	+	+	–	–
28	M	Total nephrectomy	55	Left	Y	0.6	ND	N	–	NED	56	+	–	–	w
29	F	Partial Nehprectomy	68	Right	N	10	ND	N	–	NED	36	+	NP	–	–
30	F	Partial Nehprectomy	58	Left	N	1.1	p.G12V (c.35 G > T)	Y	ChRCC (3.8 CM; KRAS wild-type)	NED	45	+	w	–	–
31	F	Total nephrectomy	71	Right	N	3.9	ND	Y	ChRCC (4.5 CM; KRAS wild-type)	–	–	NP	NP	–	–
32	F	Total nephrectomy	64	Right	N	30	p.G12R (c.34 G > C)	N	PRNRP (1 cm)	–	–	+	+	–	–
33	-	Partial Nehprectomy	–	–	–	16	p.G12V (c.35 G > T)	–	–	–	–	+	+	–	w
34	F	Partial Nehprectomy	72	Left	N	9	ND	–	–	NED	24	NP	NP	NP	NP
35	F	Partial Nehprectomy	62	Right	N	0.6	ND	Y	CCRCC (3.2 CM)	NED	30	+	+	–	–
36	F	Partial Nehprectomy	63	Left	N	1.5	ND	Y	Oncocytoma (2.3 CM)	NED	7	+	+	–	w
37	M	Total nephrectomy	58	Left	Y	0.8	ND	N	-	NED	22	+	+	–	–

Table 1. continued

	Gender	Procedure	Age	Laterality	ESRD/ CKD	Size (mm)	KRAS status	Multiple tumors	Assocaited tumor type (Size; KRAS status)	Outsome	Follow up duration (Months)	Immunohistochemistry			
												GATA-3	L1CAM	VIMENTIN	AMACR
38	M	Total nephrectomy	72	Left	Y	0.9	ND	Y	Multiple bilateral PAs	NED	30	+	NP	–	–
39	M	Total nephrectomy	74	Left	Y	1.8	p.G12V (c.35 G > T)	N	C/L UC of renal pelvis and PCa	NED	1	+	+	–	–
40	M	Total nephrectomy	71	Left	Y	0.6	p.G12V (c.35 G > T)	Y	Right sided ACD-RCC (0.9 CM)	NED	10	+	+	–	m
41	=	Total nephrectomy	=	Right	=	0.2	ND	=	–	=	=	+	+	–	m
42	F	Partial Nehprectomy	79	Right	N	16	p.G12V (c.35 G > T)	N	–	NED	13	+	+	–	w
43	F	Total nephrectomy	68	Right	Y	1.7	p.G12V (c.35 G > T)	Y	ACD-RCC (0.8 CM; KRAS wild-type); CCPRCC (1.5 CM; KRAS wild-type); AML (0.6 CM; KRAS wild-type)	NED	16	+	+	–	–
44	=	=	=	=	Y	9	p.G12V (c.35 G > T)	=	=	=	=	+	+	–	–
45	M	Total nephrectomy	71	Right	N	1.5	p.G12V (c.35 G > T)	Y	URCC (5.5 CM)	NED	1	+	+	–	–
46	F	Partial Nehprectomy	72	Left	Y	10	p.G12V (c.35 G > T)	N	–	NED	12	+	+	–	w
47	M	Total nephrectomy	73	Left	N	4.3	ND	Y	PRCC (5.5 CM)	DOC	3	+	+	–	–
48	M	Partial Nehprectomy	58	Right	N	9	p.G12V (c.35 G > T)	Y	PRCC (4.5 CM)	NED	15	+	+	–	w/m
49	M	Renal Biopsy	68	Left	N	30	p.G12D (c.35 G > A)	N	-	NED	4	+	+	–	w
50	F	Partial Nehprectomy	68	Right	N	21	p.G12R (c.34 G > C)	N	-	NED	8	+	+	–	–

M male, *F* female, *ESRD/CKD* end stage renal disease/chronic kidney disease, *PRCC* papillary renal cell carcinoma, *CCRCC* clear cell RCC, *PA* papillary adenoma, *ACD-RCC* acquired cystic disease-associated RCC, *ChRCC* chromophobe RCC, *PRNRP* papillary renal neoplasm with reverse polarity, *URCC* unclassified renal cell carcinoma, *C/L* contralateral, *UC* urothelial carcinoma, *PCa* prostatic carcinoma, *NED* no evidance of disease, *DOC* died of other causes, *NP* not performed, *w* weak, *m* moderate. - not available/applicable, = the same patient in the above row.

DISCUSSION

We recently introduced the term "papillary renal neoplasm with reverse polarity (PRNRP)" to describe a subset of renal epithelial tumors with characteristic features. In the original series, we found distinctive morphologic and immunohistochemical features that set this tumor aside from other described renal cell carcinomas, including papillary renal cell carcinoma (PRCC). Our original series included radiologically detected masses and found alterations of the *KRAS* molecular pathway in 9 of 10 analyzed cases while none of the control series of PRCCs had these mutations. In the current study, in which we deliberately focused on clinically undetected and incidental neoplasms, we identified recurrent *KRAS* mutations in neoplasms as small as 0.6 mm, although the mutation detection rate was higher in those measuring ≥1 mm. Chang et al[6] have attributed this to the limited tumor content. However, considering that our clinical assay is routinely used for the detection of mutations in small tumor contents from cytology samples, this is unlikely. However, using more sensitive assays such as digital droplet PCR might be useful to address this tumor content issue.

We used the term "reverse polarity" for this entity to indicate the consistently unusual nuclear localization toward the apical end of the cell as we discussed in detail in our original study[1]. Additionally, we intentionally avoided the use of descriptive terminology related to the cytoplasmic staining "eosinophilic or oncocytic" because the acquisition of more knowledge about this entity may identify different cytoplasmic qualities, either focally or non-focally. For instance, "chromophobe" renal cell carcinoma is a term used to this day, which means a "hard to stain"[18], which later on had led to the addition of the "eosinophilic" prefix to some of these tumors. Of note, we identified focal clear cell changes in 3 neoplasms in the current series, a finding described recently by Chang et al as well[6]. Moreover, we did not use such descriptive terminology to avoid lumping it with the prior studies which showed a wide range of morphologic and immunohistochemical features to what has been described as "oncocytic papillary renal cell carcinoma". Therefore, we believe that it is best to maintain

Table 2. A summary of the clinical and pathologic features of the papillary renal neoplasm with reverse polarity cohort.

Parameter	Clinically undetected	Clinically detected
Age (years)		
Range	33–84	45–79
Mean	64	62
Median	65	64
Gender		
Male	17/31 (55%)	4/16 (25%)
Female	14/31 (45%)	12/16 (75%)
Laterality		
Right	15/33 (45%)	9/12 (75%)
Left	18/33 (55%)	3/12 (25%)
Size (mm)		
Range	0.2–4.3	9–30
Mean	1.4	16
Median	1.1	13
IHC		
GATA3	32/32 [100% (1 = weak)]	15/15 (100%)
L1CAM	22/26 [85% (6 = weak)]	12/12 (100%)
AMACR	6/32 [19% (4 = weak; 2 = moderate)]	6/14 [43% (5 = weak; 1 = weak-moderate)]
Vimentin	0/32 (0%)	0/12 (0%)

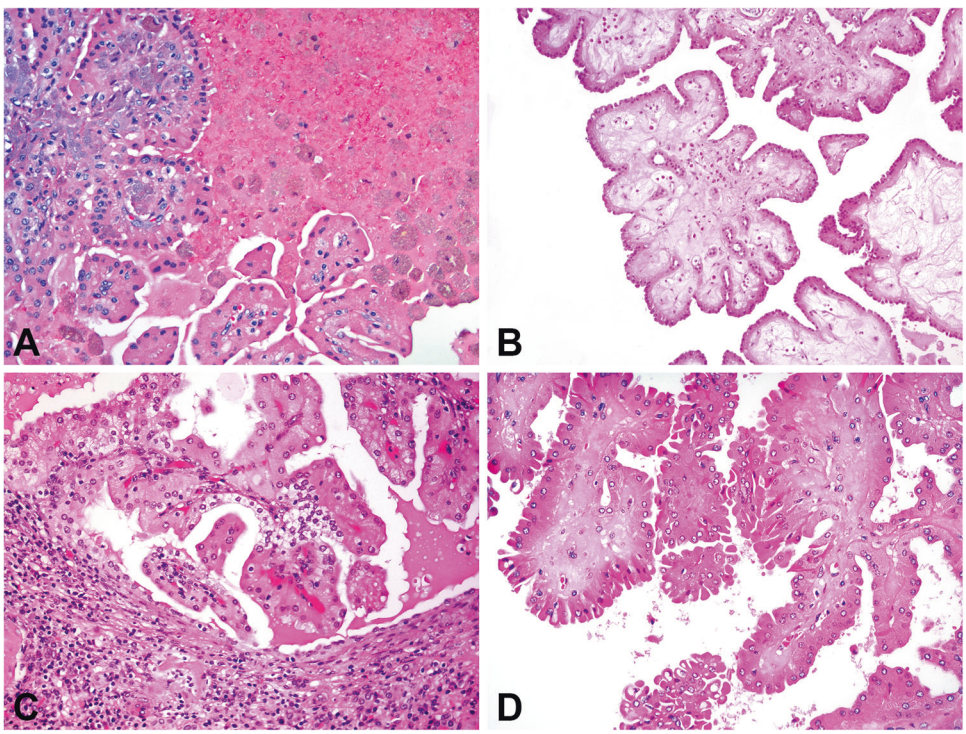

Fig. 1 Unusual features of papillary renal neoplasm with reverse polarity. These include cystic neoplasm filled with eosinophilic proteinaceous material containing loose hemosiderin-laden macrophages and cellular debris (**A**), edematous and expanded fibrovascular cores containing chronic inflammatory infiltrates (**B**), focal clear cell changes (**C**), and hobnail conformation (**D**).

the "papillary renal neoplasm with reverse polarity" terminology for these distinct neoplasms, and also to avoid terminological differences in future studies.

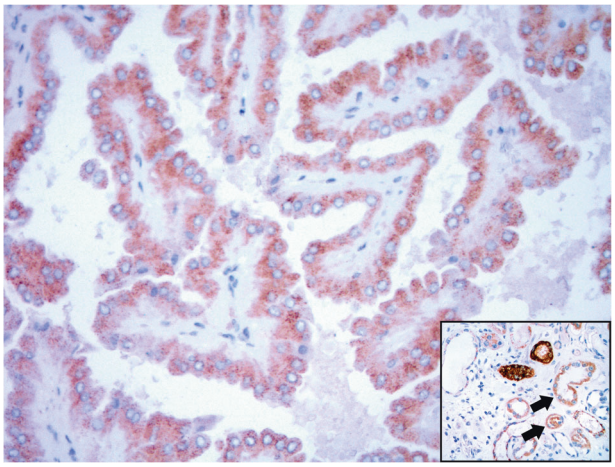

Fig. 2 Immunohistochemical reaction for AMACR. AMACR staining showing weak to moderate reaction, with similar intensity to that observed in the distal convoluted tubules and collecting ducts and less than the proximal convoluted tubules (inset; arrows are pointing out the distal convoluted tubules).

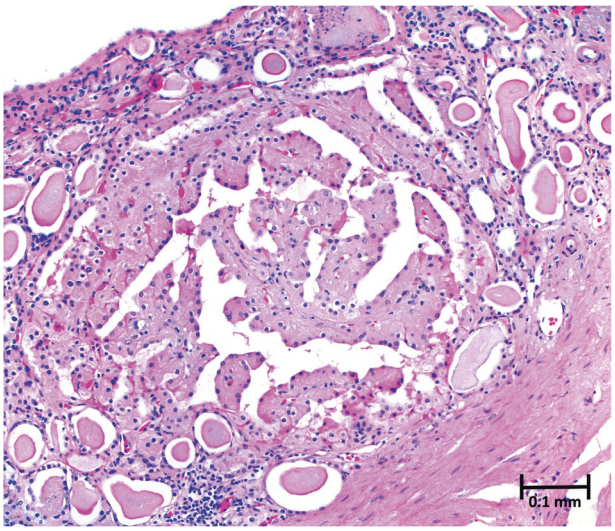

Fig. 3 Microscopic papillary renal neoplasm with reverse polarity. A representative image of the smallest (0.6 mm) papillary renal neoplasm with reverse polarity with detected *KRAS* mutation in the current series.

Including this series, 158 such neoplasms have been reported with marked consistency in the morphology, despite small variations and some features that were not mentioned in our original series, including focal hobnail conformation and focal clear cell changes. Additionally, a recent paper by Wei et al documented that these neoplasms may be cystic[10]. The cysts are usually filled with proteinaceous fluid or blood and may contain floating degenerated cells and filled with hemosiderin. The appearance of thick intracystic proteinaceous fluid or blood may be confused with necrosis, however, true tumor type coagulative necrosis is absent in these neoplasms.

The immunohistochemical profile of PRNRP is consistent. They are consistently positive for GATA3 and keratin 7 and are negative for vimentin. The presence of focal weak positive reaction for vimentin reported in 6% (7/118)[7,19] is highly atypical; the interpretation of vimentin staining may sometimes be difficult, particularly when the fibrovascular cores are compressed or fibrotic resulting in a false-positive reaction. One PRNRP was reported to show focal reaction with anti-CD117 (KIT) antibody[10], however, as observed by Chang et al, these neoplasms may contain mast cells within the fibrovascular cores, and if prominent, they may give an impression of a positive reaction[6]. Lastly, although these neoplasms typically lack the increased immunoexpression of α-methylacyl-CoA-racemase (AMACR), it is not unusual to see weak cytoplasmic blush or even, in rare instances, moderate reactivity. In these scenarios, however, the expression of AMACR appears to match the expression seen in the distal rather than proximal convoluted tubules, which may serve as internal control when assessing the immunoexpression of AMACR in these neoplasms.

In the recent paper by the Genitourinary Pathology Society (GUPS), it was suggested that the PRNRP represents a subtype of PRCC along with the biphasic, solid, Warthin-like tumors[3]. Structurally, although both PRCC and PRNRP have predominantly papillary architecture, the presence of papillary structures is not restricted to PRCC and can be prominent in other tumors, including clear cell papillary renal cell carcinoma, hereditary leiomyomatosis and renal cell carcinoma-associated renal cell carcinoma (HLRCC), and MiT-Family translocation renal cell carcinoma. The positive immunohistochemical reactions for GATA3 and L1CAM, the increased mRNA expression of these genes, as well as the negative reactions for vimentin and, to less extent, AMACR, are features that contrast with PRCC including the other suggested subtypes. Additionally, the shared chromosome 7 and/ or 17 trisomy and/ or deletion of Y chromosome in males, that we identified in our original series, is not limited to PRCC and PRNRP, but was also reported in 30–40% of HLRCC and tubulocystic carcinoma[20–23]. Moreover, the presence of *KRAS* mutations was proven by multiple independent studies to be unique and consistent in PRNRP (mutational detection rate was up to 93% in some studies); therefore, the presence of *KRAS* mutations in other tumors [0.6% (n = 2/290) of the papillary renal

Table 3. A summary of the KRAS mutation status of the papillary renal neoplasm with reverse polarity cohort.

Category		Clinically undetected		Clinically detected
Size range (n)		**< 1 mm (n = 15)**	**≥ 1-4.3 mm (n = 19)**	**9-30 mm (n = 16)**
KRAS mutation		1 (7%)	14 (74%)	14 (88%)
Variant	p.G12V (c.35 G > T)	1	11	9
	p.G12D (c.35 G > A)	0	1	1
	p.G12C (c.34 G > T)	0	2	1
	p.G12R (c.34 G > C)	0	0	2
	p.G12A/V/D complex mutation	0	0	1

N number of neoplasms.

cell carcinomas "KIRP" TCGA cohort] is likely to represent a random rather than a recurrent event. This finding was also supported by all studies of the PRNRP that included PRCC in their control group, which have shown a negative *KRAS* mutational status (wild-type). In the same notion, a significant proportion of the low-grade oncocytic tumor, eosinophilic vacuolated tumor, eosinophilic solid and cystic renal cell carcinoma, renal cell carcinoma with leiomyomatous stroma, and acquired cystic disease-associated renal cell carcinoma share TSC/MTOR pathways mutations at a rate that far exceeds the "shared" *KRAS* mutational rate between PRNRP and any other tumor described thus far, including PRCC; however, all of the aforementioned tumors are considered different entities. Lastly, in our previous study, we performed unsupervised mRNA clustering of 17 tumors obtained from the Cancer Genome Atlas (3 PRNRP, the 2 *KRAS* mutated PRCCs, and 12 randomly selected PRCCs) and those showed different expression profiles of PRNRP when compared to other tumors[2].

In summary, the presence of *KRAS* mutations in small, clinically undetectable (microscopic) neoplasms suggests a distinct oncogenic pathway for PRNRP as these mutations appear to be an early events in their genesis.

REFERENCES

1. Al-Obaidy, K. I. et al. Papillary renal neoplasm with reverse polarity: a morphologic, immunohistochemical, and molecular study. *Am. J. Surg. Pathol.* **43**, 1099–1111 (2019).
2. Al-Obaidy, K. I. et al. Recurrent *KRAS* mutations in papillary renal neoplasm with reverse polarity. *Mod. Pathol* **33**, 1157–1164 (2020).
3. Trpkov, K. et al. New developments in existing WHO entities and evolving molecular concepts: the Genitourinary Pathology Society (GUPS) update on renal neoplasia. *Mod Pathol* **34**, 1392–1424 (2021).
4. Kunju, L. P., Wojno, K., Wolf, J. S. Jr, Cheng, L. & Shah, R. B. Papillary renal cell carcinoma with oncocytic cells and nonoverlapping low grade nuclei: expanding the morphologic spectrum with emphasis on clinicopathologic, immunohistochemical and molecular features. *Hum. Pathol* **39**, 96–101 (2008).
5. Saleeb, R. M. et al. Toward biological subtyping of papillary renal cell carcinoma with clinical implications through histologic, immunohistochemical, and molecular analysis. *Am. J. Surg. Pathol.* **41**, 1618–1629 (2017).
6. Chang, H. Y. et al. Clinicopathological and molecular characterisation of papillary renal neoplasm with reverse polarity and its renal papillary adenoma analogue. *Histopathology* **78**, 1019–1031 (2021).
7. Kim, S. S. et al. Recurrent *KRAS* mutations identified in papillary renal neoplasm with reverse polarity-a comparative study with papillary renal cell carcinoma. *Mod Pathol* **33**, 690–699 (2020).
8. Kiyozawa, D. et al. Morphological, immunohistochemical, and genomic analyses of papillary renal neoplasm with reverse polarity. *Hum Pathol* **112**, 48–58 (2021).
9. Lee, H. J. et al. Unilateral synchronous papillary renal neoplasm with reverse polarity and clear cell renal cell carcinoma: a case report with *KRAS* and *PIK3CA* mutations. *Diagn. Pathol* **15**, 123 (2020).
10. Wei, S. et al. Papillary renal neoplasm with reverse polarity is often cystic: report of 7 cases and review of 93 cases in the literature. *Am. J. Surg. Pathol.* https://doi.org/10.1097/PAS.0000000000001773 (2021). Online ahead of print.
11. Zhou, L. et al. Papillary renal neoplasm with reverse polarity: a clinicopathologic study of 7 cases. *Int. J. Surg. Pathol.* **28**, 728–734 (2020).
12. Tong, K. et al. Frequent *KRAS* mutations in oncocytic papillary renal neoplasm with inverted nuclei. *Histopathology* **76**, 1070–1083 (2020).
13. Brunelli, M., Eble, J. N., Zhang, S., Martignoni, G. & Cheng, L. Gains of chromosomes 7, 17, 12, 16, and 20 and loss of Y occur early in the evolution of papillary renal cell neoplasia: a fluorescent in situ hybridization study. *Mod Pathol* **16**, 1053–1059 (2003).
14. Calio, A., Warfel, K. A. & Eble, J. N. Papillary adenomas and other small epithelial tumors in the kidney: an autopsy study. *Am. J. Surg. Pathol.* **43**, 277–287 (2019).
15. Al-Obaidy, K. I. et al. Recurrent *KRAS* mutation is an early event in the development of papillary renal neoplasm with reverse polarity (abstract 1865). *Mod Pathol* **33**, 1002–1163 (2020).
16. Mantilla, J. G., Antic, T. & Tretiakova, M. GATA3 as a valuable marker to distinguish clear cell papillary renal cell carcinomas from morphologic mimics. *Hum Pathol* **66**, 152–158 (2017).
17. Priemer, D. S., Vortmeyer, A. O., Zhang, S., Chang, H. Y., Curless, K. L. & Cheng, L. Activating *KRAS* mutations in arteriovenous malformations of the brain: frequency and clinicopathologic correlation. *Hum Pathol* **89**, 33–39 (2019).
18. Thoenes, W., Storkel, S. & Rumpelt, H. J. Human chromophobe cell renal carcinoma. *Virchows Arch. B Cell Pathol. Incl. Mol. Pathol.* **48**, 207–217 (1985).
19. Pivovarcikova, K. et al. Renal cell carcinomas with tubulopapillary architecture and oncocytic cells: Molecular analysis of 39 difficult tumors to classify. *Ann. Diagn. Pathol.* **52**, 151734 (2021).
20. Koski, T. A. et al. Array comparative genomic hybridization identifies a distinct DNA copy number profile in renal cell cancer associated with hereditary leiomyomatosis and renal cell cancer. *Genes Chromosomes Cancer* **48**, 544–551 (2009).
21. Pivovarcikova, K. et al. Fumarate hydratase deficient renal cell carcinoma and fumarate hydratase deficient-like renal cell carcinoma: Morphologic comparative study of 23 genetically tested cases. *Cesk Patol* **55**, 244–249 (2019).
22. Chen, N. et al. Gains of chromosomes 7 and 17 in tubulocystic carcinoma of kidney: two cases with fluorescence in situ hybridisation analysis. *J. Clin. Pathol.* **67**, 1006–1009 (2014).
23. Sarungbam, J. et al. Tubulocystic renal cell carcinoma: a distinct clinicopathologic entity with a characteristic genomic profile. *Mod. Pathol* **32**, 701–709 (2019).

AUTHOR CONTRIBUTIONS

K.I.A., J.N.E., D.J.G., and L.C. performed study concept, methodology, design and writing; R.M.S, T.K., S.R.W., A.R.S, O.H., R.M., A.C., A.M.A, Z.I.A, O.H., N.G., A.O.O., W.A.S. J.N.E., D.J.G., and L.C. provided case material, K.I.A and A.A. provided acquisition of data. K.I.A., R.M.S, T.K., J.N.E., and L.C. participated in manuscript drafting. J.D.S and L.A.B. provided technical and material support. All authors reviewed and approved the manuscript.

COMPETING INTERESTS

The authors declare no competing interests.

ETHICS APPROVAL AND CONSENT TO PARTICIPATE

This study was approved by the Institutional Review Board (IRB) at Indiana University, Indianapolis, USA, under protocol number: 1301010350. Ethical approval for this study was waived.

ADDITIONAL INFORMATION

Correspondence and requests for materials should be addressed to Liang Cheng.

Reprints and permission information is available at http://www.nature.com/reprints

Publisher's note Springer Nature remains neutral with regard to jurisdictional claims in published maps and institutional affiliations.